A Dynamic Model for the Energy Management of Microgrid-Enabled Production Systems

Wester C.H. Schoonenberg[a,*], Amro M. Farid[a]

[a]*Thayer School of Engineering at Dartmouth, 14 Engineering Drive Hanover, NH 03755, USA*

Abstract

In recent years, industrial facilities are devoting ever greater attention to the importance of energy in their operations. It directly supports the challenges of high availability, quality excellence, and compliance with ever more ambitious sustainability targets. Such objectives are often beyond the scope of local electric utilities, and so this work, instead, considers *microgrid-enabled production systems*. In such a case, the production enterprise is motivated to in-source its energy supply so as to tailor its management and delivery to the needs of its production system. The introduction of microgrids to a production system setting opens several new industrial energy management activities. Here, the microgrid's dynamic power balancing activities in the operations time scale are of greatest importance. The power supply, which may potentially be variable, must be matched to the industrial loads which are a byproduct of production activities. Therefore, this article seeks to develop a Dynamic Energy Management Model for Microgrid-Enabled Production Systems. The model is based on a *hetero-functional graph theory* rooted in the Axiomatic Design for Large Flexible Engineering Systems and timed Petri nets. The static stability of the microgrid is analyzed using power flow analysis. The resulting model is applied to an illustrative example in which a multi-resource production system is coupled to a microgrid with several types of power generation. The outcomes of the example show that the variable electricity demand imposed by production activities is ill accommodated by renewable energy sources alone. Consequently, the stability of the microgrid is maintained by a dispatchable generator. This holistic model, therefore, includes the impact of the production schedule on greenhouse gas emissions.

Keywords: Demand Response, Axiomatic Design, petri net model, manufacturing system, smart grid, multi-layer networks

Nomenclature

$()^V$	Vectorization of a matrix, equivalent to *vec*( )	ϵ_{xl_i}	Action or event in the product net of product l_i
$\cdot$	Hadamard product	$\Lambda_{\mu i}$	Product transformation feasibility matrix
$\circledast$	Aggregation operator	$\mathbf{0}^{\sigma(n)\times\sigma(m)}$	Zeros matrix of size $\sigma(n) \times \sigma(m)$

V	Vector of nodeal voltage levels	H	Set of transporting resources
Y	Bus admittance matrix	H_{MG}	The set of Transmission Lines
$\mathbb{1}^n$	column ones vector of predefined length n	H_{PS}	The set of Material Handlers
$\mathbb{P}$	Projection operator	i	Index for DOF ψ_i in set $\mathcal{E}_S$
$\mathbb{P}_H$	Projection matrix	j	Index for transformation process $p_{\mu j}$ in set P_μ
$\mathbb{P}_M$	Projection matrix	J_φ	Holding knowledge base
$\odot$	Matrix boolean multiplication	J_H	Transportation knowledge base
$\ominus$	Matrix boolean subtraction	J_M	Transformation knowledge base
$\otimes$	Kronecker product	J_S	System Knowledge Base
Φ	State transfer function dependent on $Q_B[k]$ and $U[k]$	$J_{\tilde{H}_{MG}}$	Microgrid refined transportation knowledge base
Φ_T	State transition function dependent on $Q[k]$, $U^-[k]$, and $U^+[k]$	$J_{\tilde{H}_{MPS}}$	Microgrid-Enabled Production System refined transportation knowledge base
ψ_i	DOF i in the set of structural degrees of freedom $\mathcal{E}_S$	$J_{\tilde{H}_{PS}}$	Production system refined transportation knowledge base
$\sigma()$	The size of the set ()	$J_{\tilde{H}}$	Refined transportation knowledge base
θ_ψ	The associated voltage angle relative to a predefined reference bus	$J_{\varphi_{MG}}$	Microgrid holding knowledge base
		$J_{\varphi_{PS}}$	Production system holding knowledge base
$\tilde{J}_{M_{MG}}$	Microgrid transformation knowledge base unrelated to production	$J_{H_{MG}}$	Microgrid transportation knowledge base
$\tilde{M}_{MG}$	The set of Microgrid generators and loads unrelated to production	$J_{H_{PS}}$	Production system transportation knowledge base
		$J_{M_{MG}}$	Microgrid transformation knowledge base
$\tilde{P}_{\mu MG}$	The set of microgrid generating and consuming processes unrelated to production	$J_{M_{MPS}}$	Microgrid-Enabled Production System transformation knowledge base
$\underline{R}$	Set of aggregated resources	$J_{M_{PS}}$	Production system refined transformation knowledge base
$\underline{r}_a$	Aggregated resource a in set $\underline{R}$	J_{MG}	Microgrid Knowledge Base
a	Index for aggregated resource $\underline{r}_a$ in set $\underline{R}$	J_{PS}	Production System Knowledge Base
$A_{i,j}$	Matrix used for the product transformation feasibility matrix	K_S	System constraints matrix
		l_i	Index for product
B	Set of independent buffers	M	Set of transforming resources
B_S	Set of buffers	$M^+_{\mathcal{E}_{\psi H}}$	Positive transportation degree of freedom incidence matrix
B_{MG}	The set of Substations & Storage	$M^-_{\mathcal{E}_{\psi H}}$	Negative transportation degree of freedom incidence matrix
B_{PS}	The set of Independent Input & Output Buffers	M^+_H	Incidence "in" matrix
$B_{S_{PS}}$	The set of Production system buffers	M^-_H	Incidence "out" matrix
b_{sy}	Buffer y in set B_S	M_{MG}	The set of Generators & Loads
C_C	capacity vector of size $\sigma(\mathcal{E}_S) \times 1 \in \mathbb{N}^{\sigma(\mathcal{E}_S)}$	M_{MPS}	The set of Microgrid-Enabled Production System transformation resources
d_ψ	Event duration of action ψ	M_{PS}	The set of Machines
DOF_S	The number of structural degrees of freedom	$M_{\mathcal{E}_{\psi H}}$	Transportation degree of freedom incidence matrix
e^n_i	i^{th} elementary basis vector of predefined length n	P	Set of system's processes
e_{wv}	Action in the SysML sense	P_η	Set of transportation processes
g	Index for holding process $p_{\varphi g}$ in set P_φ	P_μ	Set of transformation processes
g_ψ	Complex power assigned to the structural degree of freedom ψ	P_ψ	The active power injection from ground

P_φ	Set of holding processes	$U_{l_i}[k]$	Binary product net firing vector corresponding with product l_i at time k
p_w	System process w in set P	v	Index for system resource r_v in set R
$P_{\bar\eta PS}$	The set of Production System refined transportation processes	v_ψ	The associated voltage magnitude relative to ground
$P_{\bar\eta}$	Refined transportation processes	W	Weighting function on arcs
$P_{\eta MG}$	The set of Microgrid Transportation Processes	w	Index for system process p_w in set P
$P_{\eta PS}$	The set of Production System Transportation Processes	$w_{E\psi}$	The set of algebraic state variables in the microgrid
$p_{\eta u}$	Transportation process u in set P_η	W_{l_i}	Weighting function on product arcs
$p_{\mu j}$	Transformation process j in set P_μ	y	Index for Buffer b_{sy} in set B_S
$P_{\mu MG}$	The set of Microgrid Transformation Processes	$y_{\psi h}$	An admittance assigned to the transportation structural degree of freedom
$P_{\mu MPS}$	The set of Microgrid-Enabled Production System transformation processes	y_ψ^*	An admittance assigned to the structural degree of freedom ψ
$P_{\mu PS}$	The set of Production System Transformation Processes	$\mathcal{A}$	Aggregation matrix
$p_{\varphi g}$	Holding process g in set P_φ	$\mathcal{E}_S$	Set of events, transitions, or structural degrees of freedom
$P_{\varphi MG}$	The set of Microgrid Holding Processes	$\mathcal{E}_{\psi H}$	Power system transportation degrees of freedom
$P_{\varphi PS}$	The set of Production System Holding Processes	$\mathcal{E}_{\psi M}$	Power system transformation degrees of freedom
P_{MG}	The set of microgrid processes	$\mathcal{E}_{l_i}$	Set of product events that describe the transformation of the product between product places
P_{PS}	The set of production system processes		
$Q[k]$	Petri net marking vector, $Q[k] = [Q_B[k]; Q_\mathcal{E}[k]]$	$\mathcal{M}$	Petri net incidence matrix of size $\sigma(B_S) \times \sigma(\mathcal{E}_S)$
Q_ψ	The associated reactive power injection from ground	$\mathcal{M}^+$	Positive (ingoing) Petri net incidence matrix $(w(e_{wv}, b_y))$
$Q_B[k]$	Marking (or discrete state) vector of size $\sigma(B_S) \times 1$	$\mathcal{M}^-$	Negative (outgoing) Petri net incidence matrix $(w(b_y, e_{wv}))$
$Q_\mathcal{E}[k]$	Transition state marking vector of size $\sigma(\mathcal{E}_S) \times 1$	$\mathcal{M}_E$	Matrix that introduces degrees of freedom in Power Flow Analysis
$Q_{l_i}[k]$	Marking vector that describes the product's evolution at time step k	$\mathcal{M}_{l_i}$	Product arc relations that describe which products or components receive which product events
R	Set of system's resources		
r_v	System resource v in set R	$\mathcal{M}_{PN}$	Set of arcs from places to transitions and from transitions to places in the Petri net graph.
R_{PS}	The set of Production system resources		
S_{l_i}	Set of product places for product l_i that represents a product component at a raw, work-in-progress, or final stage of production	$\mathcal{M}_{PS}^+$	Positive (ingoing) production system incidence matrix
		$\mathcal{M}_{PS}^-$	Negative (outgoing) production system incidence matrix
t_κ	Time at time step $t_k + d_\psi$	$\mathcal{N}_{l_i}$	Product petri net for product l_i
t_k	Time at time step k	$\mathcal{S}$	Marked Petri Net (Graph)
u	Index for transportation process $p_{\eta u}$ in set P_η	$\mathscr{S}$	Scheduled Event List
$U[k]$	Binary firing vector of size $\sigma(\mathcal{E}_S) \times 1$	$\mathcal{U}[k]$	Binary product firing matrix at time step k of size $\sigma(\mathcal{E}_S) \times \sigma(L)$
$U^+[k]$	Binary input firing vector of size $\sigma(\mathcal{E}_S) \times 1$		
$U^-[k]$	Binary output firing vector of size $\sigma(\mathcal{E}_S) \times 1$	$\mathcal{Y}$	Transportation degree of freedom admittance matrix
$u_\psi[k]$	Elements in the firing vector at associated times t_k	$u_{\psi,l}[k]$	Element of product firing matrix $\mathcal{U}[k]$

Word count: 6846

3

1. Introduction

Industrial facilities are devoting ever greater attention to the importance of energy in their operations [1]. In some cases, industrial processes are energy intensive [2]. In other cases, such as with electric drives and motors, the energy supply must be of a very high quality [3]. Finally, many industrial companies are increasingly concerned with decarbonization either as imposed by regulation [4, 5], or stimulated by corporate social responsibility [6, 7]. To that end, onsite distributed renewable energy are often integrated. The combined objectives of high availability, quality and sustainability are often beyond the capabilities of the local utility and so this work considers *microgrid-enabled production systems* where the production enterprise has decided to in-source its energy supply so as to tailor its management and delivery to the needs of its production system. Microgrids have the potential to reduce local costs, energy losses, and greenhouse gases while enhancing energy reliability [8–10]. They also give owners the necessary autonomy to operate islanded from the local electric utility.

The introduction of microgrids to a production system setting opens several new industrial energy management activities in both planning and operations [11]. Energy planning focuses on energy efficiency. This static energy management approach optimizes the production system before it has been built, or when new technologies are incorporated in upgrades and retrofits [12, 13]. This not only considers production system resources, but also power systems resources, such as a microgrid infrastructure or the integration of renewable energy. Operations, or dynamic energy management, tries to optimize the usage of a given set of resources for energy consumption or cost [14, 15]. Such decisions coincide with the dynamics of the production system and may respond to several externalities, such as changes in the power grid balance, customer demand, and time-of-use prices [16–19].

Dynamic energy management is of particular importance to microgrid power balancing activities [20–24]. The trend of increasing renewable energy resources penetration in the power grid causes increases in variability and stochasticity of the power supply [25, 26]. Meanwhile, dynamic energy management controls the loads and has the potential to be a part of demand response [27, 28]. Furthermore, when operating in islanded model, the size of the microgrid limits the number of levers that control the balance; especially when the generation is stochastic. As a result, the production system and microgrid dynamics are coupled and cannot be studied separately. Energy consumption is a *byproduct* of production system activities, and the added value of energy differs per activity [29–31]. Consequently, online approaches that rely on multi-agent structures, or reactive control [32] have been developed. Meanwhile offline approaches, based on resource constraint scheduling methods or weighted multi-objective optimization have been discussed extensively [33, 34].

However, these studies do not include multi-discipline models, where the production system and microgrid dynamics are described in an unambiguous language. The need for such a multi-layer model has been discussed extensively by the network sciences community. An important remark made in [35] is that hetero-functional multi-layer models capture the interdependency and interaction of systems in a way that two separate mono-layer models cannot comprehend. This comprehension is essential to understanding structural properties such as resilience, robustness, and

4

centrality. The approach presented in this work has been already used to study the resilience of hetero-functional networks [36].

1.1. Scope

In developing a dynamic model for the energy management of microgrid-enabled production systems, the work restricts scope to discrete-part production systems. It also allows the microgrid to have a significant penetration of variable (renewable) energy resources. To ground the discussion, it is useful to consider a bird feeder manufacturing system [37–39] which is detailed later in Section 4 as an illustrative example.

Table 1: Microgrid-Enabled Production System Operations Management Decisions

Product Dispatch	When a given product part should undergo production in the facility.
Integrated Planning & Scheduling	Which sequence of processes should be used to create the product.
W.I.P. Management	When & where the product parts should be buffered.
Peak Load Management	At a given machine, when the product parts should be processed to meet the production schedule and power grid constraints.
Ancillary Services	Given the dynamics of the power grid, how can the planning & scheduling of production activities support stabilization.

The dynamic model for microgrid-enabled production systems must also be able to accommodate several operations management decisions. Such decisions, when made, serve to advance the physical state and outputs of the microgrid-enabled production system so as to achieve its operations management objectives. These are summarized in Table 1. The first decision is dispatch of product parts to different machines to undergo transforming (value-adding) processes. Second, planning and schedule determines the sequence and timing of production processes as the product parts advance through the facility. Third, it is important to actively manage where and if work-in-progress will be buffered. These three decisions are inherently coupled to the microgrid power balance. They must now also simultaneously manage the peak load constraints of the microgrid. Finally, it is possible that the operations management decisions of the production system can serve to provide ancillary services that stabilize the microgrid.

1.2. Contribution

This paper seeks to develop a dynamic model for the energy management of microgrid-enabled production systems. The goal of the model is to simultaneously analyze the flows of products in a discrete-part production system and the power flows in the coupled microgrid. The model is developed in such a way as to describe a production system and microgrid of arbitrary size, topology and coupling. The model also specifically includes renewable energy to support the objective of greater sustainability. The load balance requirements resulting from the renewable energy integration impose the need for a dispatchable generator, with related carbon emissions.

5

Meanwhile, this work advances a broader body of literature in the network sciences called *multi-layer networks* [35]. Very few works present models where the layers do not have to be aligned or of the same size. The work presented in this paper advances the theory of multi-layer networks, as a result of the aforementioned coupling of the production system and the microgrid.

The model developed here is based on a *hetero-functional graph theory* rooted in the Axiomatic Design for Large Flexible Engineering Systems[40, 41]. The approach has been used to develop measures of reconfigurability of production systems [37–39, 42]. Later it was applied to model other complex multi-layer systems such as the transportation [43–46], water [47], and power domains [48]. Several recent works also demonstrate how the theory may be applied to decision-marking; including the development of Multi-Agent System Design principles for both Future Power Systems [48] and Reconfigurable Mechatronic Systems [49].
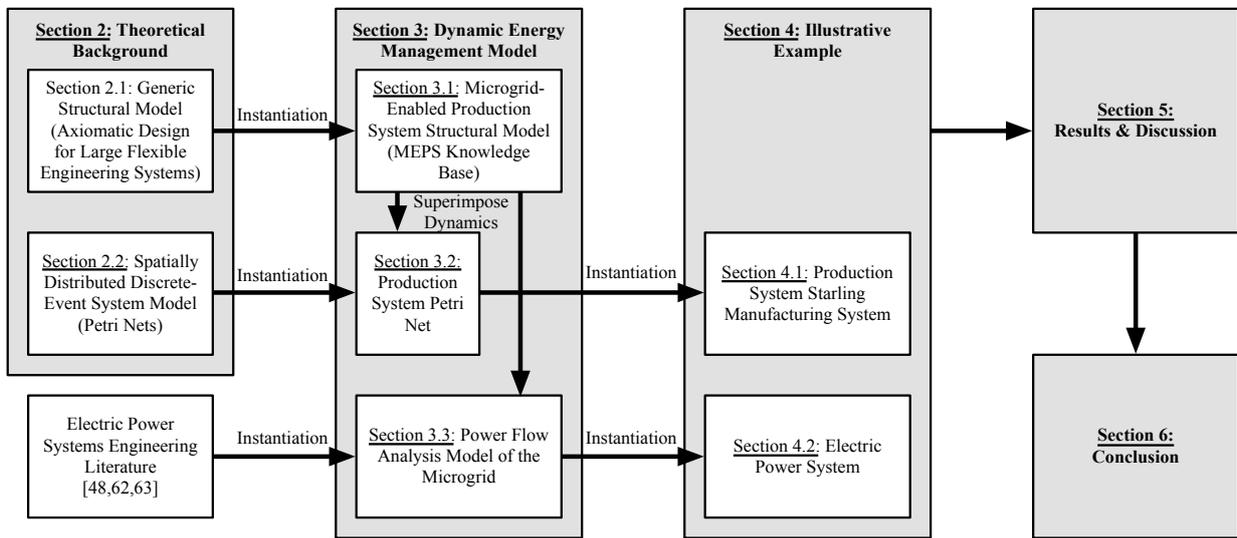

Figure 1: Visual representation of the document structure. Section numbers in top right.

Figure 1 provides an overview of the logical flow of the paper. The block elements are numbered consistently with their associated section numbers. Section 2 lays the methodological foundation of hetero-functional graph theory. Section 2.1 utilizes Axiomatic Design for Large Flexible Engineering Systems (AD4LFES) as generic model of system structure and Section 2.2 uses Petri nets as a generic model of spatially distributed discrete-event dynamics. Section 3 then develops the dynamic model for energy management by instantiation. Section 3.1 uses AD4LFES to develop a structural model of a microgrid-enabled production system. Section 3.2 and Section 3.3 then superimpose dynamics upon this structure to develop a production system petri net model and a power flow analysis model of the microgrid respectively. Section 4 introduces a case study consisting of an example production system connected to an example microgrid electric power system. Section 5 then presents and discusses the results of the case study as a validation of the model. The article is concluded with Section 6.

2. Background

The methodological foundation of this work is a hetero-functional graph theory rooted in Axiomatic Design for Large Flexible Engineering Systems and Petri nets. The former is a concise way of describing the system structure and is discussed in subsection 2.1. The latter describes the system behavior as discrete-event dynamics. It is discussed in subsection 2.2.

2.1. Axiomatic Design for Large Flexible Engineering Systems

Microgrid-enabled production systems may be classified as a Large Flexible Engineering System. This subsection recalls how Axiomatic Design treats these systems in terms of their system resources, system processes, and the allocation of the latter to the former [42, 44–50]

Definition 1. Large Flexible Engineering System (LFES) [36, 51]: an engineering system with many functional requirements that not only evolve over time, but also can be fulfilled by one or more design parameters.

Although this paper relies on an Axiomatic Design structural model, it departs from its terminology without any change in interpretation. The functional requirements and the design parameters are understood to be mutually exclusive and collectively exhaustive sets of the system's processes (P) and resources (R). As a theory, Axiomatic Design presents several advantages that are directly relevant to microgrid-enabled production systems.

These include modeling support for:

- systems of heterogeneous modes of production (but identical function)

- systems of a fundamentally hetero-functional nature.

- the allocation of system function to form.

- systems of variable structure to support reconfigurable operation.

The set of system's resources $R = M \cup B \cup H$ are classified as the set transforming resources $M = \{m_1, \ldots, m_{\sigma(M)}\}$, independent buffers $B = \{b_1, \ldots, b_{\sigma(B)}\}$, and transporting resources $H = \{h_1, \ldots, h_{\sigma(H)}\}$, with $\sigma()$ being the size of the set. For later simplicity, the set of buffers $B_S = M \cup B$ is also defined [42, 50]. Since Axiomatic Design for LFES supports modelling of complex systems, aggregating of resources R can be useful to combine different systems. The aggregation matrix $\mathcal{A}$ assigns resource r_j to aggregated resource $\underline{r}_i$ to create the set of aggregated resources $\underline{R}$ [38, 39].

$$\underline{R} = \mathcal{A} \circledast R \tag{1}$$

Definition 2. Aggregation Operator $\circledast$ [38, 39]: Given boolean matrix A and sets B and C, $C = A \circledast B$ is equivalent to:

$$C(i) = \bigcup_j a(i, j) \wedge b(j) \tag{2}$$

7

The set of system's processes P can be classified as the set of transforming, transporting, and holding processes.

Definition 3. Transformation Process[39, 42, 50]: A resource-independent, technology-independent process $p_{\mu_j} \in P_\mu = \{p_{\mu_1} \dots p_{\mu_{\sigma(P_\mu)}}\}$ that transforms an artifact from one form into another.

Definition 4. Transportation Process [39, 42, 50]: A resource-independent process $p_{\eta u} \in P_\eta = \{p_{\eta 1} \dots p_{\eta \sigma(P_\eta)}\}$ that transports artifacts from one buffer b_{sy_1} to b_{sy_2}. There are $\sigma^2(B_S)$ such processes of which $\sigma(B_S)$ are "null" processes where no motion occurs. The following convention of indices is adopted:

$$u = \sigma(B_S)(y_1 - 1) + y_2 \tag{3}$$

This convention implies a directed bipartite graph between the set of independent buffers and the transportation processes whose incidence out M_H^- and incidence in M_H^+ matrices are given by [48]:

$$M_H^- = \sum_{y1=1}^{\sigma(B_S)} e_{y1}^{\sigma(B_S)} [e_{y1}^{\sigma(B_S)} \otimes \mathbb{1}^{\sigma(B_S)}]^T \tag{4}$$

$$M_H^+ = \sum_{y2=1}^{\sigma(B_S)} e_{y2}^{\sigma(B_S)} [\mathbb{1}^{\sigma(B_S)} \otimes e_{y2}^{\sigma(B_S)}]^T \tag{5}$$

where $\mathbb{1}^n$ is a column ones vector of predefined length n, e_i^n is the ith elementary basis vector, and $\otimes$ is the kronecker product.

Definition 5. Holding Process [39, 42, 50]: A transportation independent process $p_{\varphi g} \in P_\varphi$ that holds artifacts during the transportation from one buffer to another.

Together, the system processes and resources address hetero-functionality in a LFES.

System processes P are allocated to system resources R via the system knowledge base J_S. The Axiomatic Design equation describes the allocation [39, 42, 50]:

$$P = J_S \odot R \tag{6}$$

where $\odot$ is matrix boolean multiplication and J_S is defined as:

Definition 6. System Knowledge Base [39, 42, 50]: A binary matrix J_S of size $\sigma(P) \times \sigma(R)$ whose element $J_S(w, v) \in \{0, 1\}$ is equal to one when action e_{wv} (in the SysML sense [52]) exists as a system process $p_w \in P$ being executed by a resource $r_v \in R$.

The system knowledge base J_S is constructed based on the smaller knowledge bases that address transformation, transportation and holding processes individually.

$$P_\mu = J_M \odot M$$
$$P_\eta = J_H \odot R$$
$$P_\varphi = J_\varphi \odot R \tag{7}$$

8

J_S then becomes [39, 42, 50]:

$$J_S = \left[\begin{array}{c|c} J_M & \mathbf{0} \\ \hline J_{\bar{H}} \end{array} \right]$$

(8)

where in order to account for the simultaneity of holding and transportation processes into refined transportation processes $P_{\bar{\eta}}$ [39, 42, 50]:

$$J_{\bar{H}} = \left[J_\varphi \otimes \mathbb{1}^{\sigma(P_\eta)} \right] \cdot \left[\mathbb{1}^{\sigma(P_\varphi)} \otimes J_H \right]$$

(9)

where $\cdot$ is the hadamard product.

The system knowledge base has an additional property in that it defines the LFES structural degrees of freedom. These are important in the construction of the dynamic system state vector in large complex systems.

Definition 7. Structural Degrees of Freedom [39, 42, 50]: The set of independent actions $\psi_i \in \mathcal{E}_S$ that completely defines the available processes in a LFES. Their number is given by:

$$DOF_S = \sigma(\mathcal{E}_S) = \sum_w^{\sigma(P)} \sum_v^{\sigma(R)} J_S(w, v) \ominus K_S(w, v)$$

(10)

where $\ominus$ is boolean subtraction and K_S is a constraints matrix of appropriate size that eliminates actions from the action set. It serves to distinguish between the existence and the availability of a degree of freedom. For example, scheduled maintenance can disable a degree of freedom removing it from the system structure.

Previous work has applied a vectorization of the system knowledge base for mathematical convenience [48]. The shorthand $()^V$ is used to replace $vec()$. Additionally, a projection operator projects the vectorized knowledge base onto a one's vector to eliminate sparsity $\mathbb{P}J_S^V = \mathbb{1}^{\sigma(\mathcal{E}_S)}$. While solutions for $\mathbb{P}$ are not unique, this work chooses:

$$\mathbb{P} = \left[e_{\psi_1}^{\sigma(P)\sigma(R)}, \dots, e_{\psi_{\sigma(\mathcal{E}_S)}}^{\sigma(P)\sigma(R)} \right]$$

(11)

where $e_{\psi_i}^{\sigma(P)\sigma(R)}$ is the ψ_i^{th} elementary row vector corresponding to the first up to the last structural degree of freedom in increasing order.

2.2. Petri Nets

Petri nets are a concise and commonly used tool to model discrete part production system dynamics. This subsection describes their untimed and timed variants for later use.

Definition 8. Marked Petri Net (Graph)[53]: A bipartite directed graph represented as a 5-tuple $\mathcal{N} = \{B_S, \mathcal{E}_S, \mathcal{M}, W, Q_B\}$ where:

- B_S is a finite set of places of size $\sigma(B_S)$.

- $\mathcal{E}_S$ is a finite set of transitions/events of size $\sigma(\mathcal{E}_S)$.

- $\mathcal{M}_{PN} \subseteq (B_S \times \mathcal{E}_S) \cup (\mathcal{E}_S \times B_S)$ is a set of arcs of size $\sigma(\mathcal{M}_{PN})$ from places to transitions and from transitions to places in the graph.

- $W : \mathcal{M}_{PN} \to \{0, 1\}$ is the weighting function on arcs.

- Q_B is a marking (or discrete state) vector of size $\sigma(B_S) \times 1 \in \mathbb{N}^{\sigma(B_S)}$.

The arcs of the Petri net graph and its weightings define the Petri net incidence matrix.

Definition 9. Petri Net Incidence Matrix[53]: An incidence matrix $\mathcal{M}$ of size $\sigma(B_S) \times \sigma(\mathcal{E}_S)$ where:

$$\mathcal{M} = \mathcal{M}^+ - \mathcal{M}^- \tag{12}$$

where $\mathcal{M}^+(y, \psi) = w(e_{wv}, b_y)$ and $\mathcal{M}^-(y, \psi) = w(b_y, e_{wv})$ and ψ is a unique index mapped from the ordered pair (w, v).

The Petri-net structure leads directly to the definition of its discrete-event dynamics.

Definition 10. Petri Net (Discrete-Event) Dynamics[53]: Given a binary firing vector $U[k]$ of size $\sigma(\mathcal{E}_S) \times 1$ and a Petri-net incidence matrix $\mathcal{M}$ of size $\sigma(B_S) \times \sigma(\mathcal{E}_S)$, the evolution of the marking vector Q_B is given by the state transition function $\Phi(Q_B[k], U[k])$:

$$Q_B[k + 1] = \Phi(Q_B, U[k]) = Q_B[k] + \mathcal{M}U[k] \tag{13}$$

Beyond ordinary Petri nets, timed Petri as their name suggests introduce time into the dynamics definition

Definition 11. Timed Petri Net (Discrete-Event) Dynamics[54]: Given a binary input firing vector $U^+[k]$ and a binary output firing vector $U^-[k]$ both of size $\sigma(\mathcal{E}_S) \times 1$, and the positive and negative components $\mathcal{M}^+$ and $\mathcal{M}^-$ of the Petri-net incidence matrix of size $\sigma(B_S) \times \sigma(\mathcal{E}_S)$, the evolution of the marking vector Q is given by the state transition function $\Phi_T(Q[k], U^-[k], U^+[k])$:

$$Q[k + 1] = \Phi_T(Q[k], U^-[k], U^+[k]) \tag{14}$$

where $Q = [Q_B; Q_\mathcal{E}]$ and

$$Q_B[k + 1] = Q_B[k] \qquad + \qquad \mathcal{M}^+ U^+[k] \qquad - \qquad \mathcal{M}^- U^-[k] \tag{15}$$

$$Q_\mathcal{E}[k + 1] = Q_\mathcal{E}[k] \qquad - \qquad U^+[k] \qquad + \qquad U^-[k] \tag{16}$$

Note that Timed Petri Nets separate the infinitesimally short firing vector of ordinary Petri nets into distinct input and the output firing vectors separated by processing times. Q_B and $Q_\mathcal{E}$ track the location of the tokens in the production system. Q_B tracks the states of the buffers and $Q_\mathcal{E}$ the state of (ongoing) transitions [54, 55]. The transitions are fired based on a scheduled event list that combines the discrete events with a time interval.

Definition 12. Scheduled Event List[53]: A tuple $\mathcal{S} = (u_\psi[k], t_k)$ consisting of all elements $u_\psi[k]$ in firing vectors $U^-[k]$ and their associated times t_k. For every element, $u_\psi^-[k] \in U^-[k]$, there exists another element $u_\psi^+[\kappa] \in U^+[\kappa]$ which occurs at time t_κ d_ψ time units later. $t_\kappa = t_k + d_\psi$.

Table 2: System Processes & Resources in a microgrid-enabled production system[38, 39, 56]

	P_μ	P_η	P_φ	M	B	H	J_S
LFES	Transformation	Transportation	Holding	Transforming Resource	Independent Buffer	Transportation Resource	Knowledge Base
Production System	Transformation $(P_{\mu PS})$	Transportation $(P_{\eta PS})$	Holding $(P_{\varphi PS})$	Machines (M_{PS})	Input & Output Buffers (B_{PS})	Material Handlers (H_{PS})	Production System Knowledge Base (J_{PS})
Microgrid	Generation & Consumption $(P_{\mu MG})$	Transmission $(P_{\eta MG})$	Voltage Level $(P_{\varphi MG})$	Generators & Loads (M_{MG})	Substations & Storage (B_{MG})	Lines (H_{MG})	Microgrid Knowledge Base (J_{MG})

3. Model Development

This section develops the Dynamic Energy Management Model for Microgrid-Enabled Production Systems using Axiomatic Design, timed Petri-nets and physical modeling. First, a single knowledge base for the microgrid-enabled production system is constructed as a succinct description of system structure. The remainder of the section addresses the system behavior using the Axiomatic Design knowledge base as a foundation. A timed Petri-net model is derived to describe the production system's discrete event dynamics. Finally, a power flow analysis model is added as a physical model of the microgrid that allows for energy management by analyzing the system behavior [57]. The development represents a logical extension of the production system model in [58] and the transportation electrification model in [43, 45].

3.1. Microgrid-Enabled Production System Knowledge Base

This subsection constructs the Microgrid-Enabled Production System Knowledge Base as an overlapping union of two underlying knowledge bases; one for the production system and the other for the microgrid. Table 2 provides an overview of the definitions of the resources and processes for each of these systems.

3.1.1. Production System Knowledge Base

The production system knowledge base J_{PS} is constructed based on the concepts discussed in Section 2.1. First, the production system resources R_{PS} are defined as; the transformation resources M_{PS} that represent the transforming (value-adding) machines in the production system, the independent buffers B_{PS} that represent the input, output, and intermediate buffers, and the transportation resources H_{PS} that represent the material handlers that relocate product parts [39, 42, 58].The set of all buffers is also defined as $B_{S_{PS}} = M_{PS} \cup B_{PS}$. Additionally, Definitions 3, 4, and 5 are followed to define the production system's transformation $P_{\mu PS}$, transportation $P_{\eta PS}$, and holding processes $P_{\varphi PS}$, resulting in the set of production system processes: $P_{PS} = P_{\mu PS} \cup P_{\eta PS} \cup P_{\varphi PS}$. Finally, the production system processes are mapped on the production system resources [39, 42, 58]. The system knowledge base consists of a

combination of the underlying knowledge bases, using Equation 6, 8 and 9.

$$J_{PS} = \left[\begin{array}{c|c} J_{M_{PS}} & \mathbf{0} \\ \hline & J_{\bar{H}_{PS}} \end{array} \right] \tag{17}$$

where

$$J_{\bar{H}_{PS}} = \left[J_{\varphi PS} \otimes \mathbb{1}^{\sigma(P_{\eta PS})} \right] \cdot \left[\mathbb{1}^{\sigma(P_{\varphi PS})} \otimes J_{H_{PS}} \right] \tag{18}$$

3.1.2. Microgrid Knowledge Base

The power system knowledge base is constructed similarly. First, the power system resources are defined. The transformation resources M_{MG} include the systems generators and loads. The independent buffers B_{MG} represent buffering capacity in the system, such as energy storage (e.g. batteries) or buses. Substations are modeled as independent buffers without storage capacity. The transportation resources H_{MG} represent the power lines between the buses, generators, and loads [48]. Next, Definitions 3, 4, and 5 are applied to define the microgrid's system processes. The transformation processes $P_{\mu MG}$ represent the generation and consumption of power. The transportation processes $P_{\eta MG}$ represent the power flow through the system. The holding processes $P_{\varphi MG}$ represent different voltage levels as different ways of "carrying" power. These types of processes are combined in the set of microgrid processes $P_{MG} = P_{\mu MG} \cup P_{\eta MG} \cup P_{\varphi MG}$. Finally, the microgrid system processes are mapped on to its resources [48]. The system knowledge base consists of a combination of the underlying knowledge bases, using Equation 6, 8 and 9.

$$J_{MG} = \left[\begin{array}{c|c} J_{M_{MG}} & \mathbf{0} \\ \hline & J_{\bar{H}_{MG}} \end{array} \right] \tag{19}$$

where $J_{\bar{H}_{MG}} = J_{H_{MG}}$ is assumed, given that microgrids usually only retain one voltage level. Note that every transportation resource (power line) is related to two transportation processes, one for each direction. Also note that the transforming resources can realize either power generation or a consumption process but not both.

3.1.3. Microgrid Enabled Production System Knowledge Base

The Microgrid-Enabled Production System knowledge base is a union of the two previously identified knowledge bases J_{PS} and J_{MG}. However, the two systems are not mutually exclusive. The transformation resources in the power system overlap with production system's resources. The resulting transformation resources for the Microgrid-Enabled Production System (M_{MPS}) can be defined as: $M_{MPS} = R_{PS} \cup \tilde{M}_{MG} = M_{PS} \cup B_{PS} \cup H_{PS} \cup \tilde{M}_{MG}$ where $\tilde{M}_{MG}$ is taken as the set of generators, and loads unrelated to production. Similarly, the production system processes are combined with the microgrid transformation processes: $P_{\mu MPS} = P_{PS} \cup \tilde{P}_{\mu MG} = P_{\mu PS} \cup P_{\bar{\eta} PS} \cup \tilde{P}_{\mu MG}$ where $\tilde{P}_{\mu MG}$ is taken as the set of generating and consuming processes unrelated to production. In order to relate these sets of processes and resources, three mutually exclusive knowledge bases are introduced: $J_{M_{MPS}}$, $J_{\bar{H}_{MPS}}$, and $\tilde{J}_{M_{MG}}$ where:

$$P_{\mu MPS} = J_{M_{MPS}} \odot M_{PS}$$

$$P_{\bar{\eta}PS} = J_{\bar{H}_{MPS}} \odot R_{PS}$$

$$\tilde{P}_{\mu MG} = \tilde{J}_{M_{MG}} \odot \tilde{M}_{MG} \tag{20}$$

similarly to as defined in Equation 7.

Consequently, the Microgrid-Enabled Production System knowledge base J_{MPS}, as a type of large flexible engineering system, takes on the structural form of Equation 8:

$$= \left[\begin{array}{c|c} J_{M_{MPS}} & \mathbf{0} \\ \hline & J_{\bar{H}_{MPS}} \end{array} \right] \tag{21}$$

Then substituting in Equation 17 gives:

$$= \left[\begin{array}{c|c|c} J_{PS} & \mathbf{0} & \mathbf{0} \\ \hline \mathbf{0} & \tilde{J}_{M_{MG}} & \mathbf{0} \\ \hline & J_{\bar{H}_{MPS}} \end{array} \right] \tag{22}$$

A final decomposition by substitution of Equation 20 gives:

$$= \left[\begin{array}{c|c|c|c} J_{M_{PS}} & \mathbf{0} & \mathbf{0} & \mathbf{0} \\ \hline & J_{\bar{H}_{PS}} & \mathbf{0} & \mathbf{0} \\ \hline \mathbf{0} & \mathbf{0} & \tilde{J}_{M_{MG}} & \mathbf{0} \\ \hline & & J_{\bar{H}_{MPS}} & \end{array} \right] \tag{23}$$

3.2. Dynamics of the Production System Domain

This subsection uses Petri-nets to describe the discrete-event dynamics in the production system domain. Two types of Petri nets are constructed. The first is called the production system Petri net and describes the evolution of the system processes and resources of the production system as they were originally defined in the Axiomatic Design knowledge base. The second is called the product Petri net and describes the evolution of products as they evolve from raw goods into finished ones. Structurally, it is also built upon the Axiomatic Design knowledge base. Dynamically, it is synchronized with the evolution of the production system Petri net. It is worth mentioning, that at first glance, the developed Petri-nets resemble "resource-oriented Petri nets" in the literature [59]. While there are some similarities, a careful inspection reveals that the novel tie to Axiomatic Design assigns very different physical meanings to the Petri-net models. Those developed here have the added benefit of being graphically intuitive and can be validated to the axiomatic design knowledge base by inspection. The production system and product Petri nets are now discussed in turn.

3.2.1. Production System Petri Net

A discrete-part production system is governed by spatially-distributed discrete-event dynamics. Petri nets have been used extensively to model the behavior of production systems [53–55, 60, 61]. Here, a production system Petri net is defined as a timed Petri net according to Definitions 8 and 11. It is at this point that the production system knowledge base in Equation 17 is tied to the production system Petri net structure. The production system buffers B_S share notation with the production system Petri net places to emphasize their equivalence. Similarly, the Petri net transitions are equivalent to the structural degrees of freedom $\mathcal{E}_S$. Consequently, the Petri net incidence matrix in Definition 9 follows the convention in Equation 3. It may be calculated by Equation 12 where $\mathcal{M}_{PS}^-$ and $\mathcal{M}_{PS}^+$ are straightforwardly derived using Equations 4, 5 and 8.

$$\mathcal{M}_{PS}^- = \sum_{y1=1}^{\sigma(B_{S_{PS}})} e_{y1}^{\sigma(B_{S_{PS}})} \left[\mathbb{P}\left(X_{y_1}^- \right)^V \right]^T \tag{24}$$

where

$$X_{y_1}^- = \left[\begin{array}{ccc} \mathbb{1}^{\sigma(P_{\mu PS})} e_{y1}^{\sigma(B_{S_{PS}})T} & | & \mathbf{0}^{\sigma(P_{\mu PS}) \times \sigma(R_H)} \\ \hline \mathbb{1}^{\sigma(P_{\varphi PS})} \otimes e_{y1}^{\sigma(B_{S_{PS}})} & \otimes \mathbb{1}^{\sigma(B_{S_{PS}})} & \otimes \mathbb{1}^{\sigma(R_{PS})T} \end{array} \right] \tag{25}$$

$$\mathcal{M}_{PS}^+ = \sum_{y2=1}^{\sigma(B_{S_{PS}})} e_{y2}^{\sigma(B_{S_{PS}})} \left[\mathbb{P}\left(X_{y_2}^+ \right)^V \right]^T \tag{26}$$

where

$$X_{y_2}^+ = \left[\begin{array}{ccc} \mathbb{1}^{\sigma(P_{\mu PS})} e_{y2}^{\sigma(B_{S_{PS}})T} & | & \mathbf{0}^{\sigma(P_{\mu PS}) \times \sigma(R_H)} \\ \hline \mathbb{1}^{\sigma(P_{\varphi PS})} \otimes \mathbb{1}^{\sigma(B_{S_{PS}})} & \otimes e_{y2}^{\sigma(B_{S_{PS}})} & \otimes \mathbb{1}^{\sigma(R_{PS})T} \end{array} \right] \tag{27}$$

To complete the production system Petri net model, capacity constraints can be applied. A capacity vector C_C of size $\sigma(\mathcal{E}_S) \times 1 \in \mathbb{N}^{\sigma(\mathcal{E}_S)}$ limits the number of tokens within a given transition.

$$Q_{\mathcal{E}}[k] \le C_C \qquad\qquad \forall k \tag{28}$$

Each element of the input firing vectors is also constrained by the availability of the associated system resource and its capacity

$$u_\psi[k] \cdot [J_S(\omega, v) \ominus K_S(\omega, v)] < C_C(\psi) \tag{29}$$

3.2.2. Product Petri Net

In addition to the production system Petri net, a product Petri net is required to describe the evolution of products as each evolve from raw to finished state.

14

Definition 13. Product Petri Net [37–39, 58]: Given product l_i, a product net is a marked Petri net graph $\mathcal{N}_{l_i} = \{S_{l_i}, \mathcal{E}_{l_i}, \mathcal{M}_{l_i}, W_{l_i}, Q_{l_i}\}$ where:

- S_{l_i} is the set of product places that represents a product component at a raw, work-in-progress, or final stage of production.

- $\mathcal{E}_{l_i}$ is the set of product events that describe the transformation of the product between product places.

- $\mathcal{M}_{l_i} \subseteq (S_{l_i} \times \mathcal{E}_{l_i}) \cup (\mathcal{E}_{l_i} \times S_{l_i})$ is the product arc relations that describe which products or components receive which product events.

- $W_{l_i} : \mathcal{M}_{l_i} \rightarrow \{0, 1\}$ is the weighting function on product arcs.

- Q_{l_i} is a marking vector that describes the product's evolution.

where

Definition 14. Product Event: A specific transformation process that may be applied to a given product.

and the associated (untimed) state transition function follows Definition 10.

$$Q_{l_i}[k + 1] = Q_{l_i}[k] + \mathcal{M}_{l_i} U_{l_i}[k] \tag{30}$$

where $U_{l_i}[k]$ is the firing vector corresponding with product l_i at time k.

Note that a different product net is needed for each product type; each of which must be instantiated to support each individual product on the shop floor. This supports mass-customized production and the intelligent product paradigm. The interested reader is referred to the underlying references for detailed discussion [38, 56].

As expected, the production system Petri net and the product Petri net dynamics are inherently coupled. A product firing matrix is introduced to synchronize the production system Petri net firing vectors with those of the product Petri nets.

Definition 15. Product Firing Matrix[44, 45, 49]: a binary product firing matrix $\mathcal{U}[k]$ of size $\sigma(\mathcal{E}_S) \times \sigma(L)$ whose element $u_{\psi,l}[k] = 1$ when the kth firing timing triggers a product l to take structural degree of freedom ψ for action.

Additionally, a product transformation feasibility matrix is required for each product to link product events to their associated transformation processes in the production system.

Definition 16. Product Transformation Feasibility Matrix[37, 38, 49]: A binary matrix $\Lambda_{\mu i}$ of size $\sigma(\mathcal{E}_{l_i}) \times \sigma(P_\mu)$ whose value $\Lambda_{\mu i}(x, j) = 1$ iff $\epsilon_{x l_i}$ realizes transformation process $p_{\mu j}$.

Consequently, the production system input firing vectors at a given moment k become [37, 38, 49]:

$$\Lambda_{\mu i}^T \cdot U_{l_i} = A_{i,j} \cdot \mathcal{U} \cdot e_{l_i}^{\sigma(L)T} \tag{31}$$

where e_i^n represents the ith elementary basis vector of predefined length n and $A_{i,j} = 1$ if $p_{\mu i}$ is used in ϵ_{S_j}.

15

3.3. Power Flow Analysis Model of the Microgrid

To complete the dynamic energy management model for a microgrid-enabled production system, a power flow analysis model of the microgrid is introduced. To this end, the link between Axiomatic Design and power flow analysis has been previously established [48] and is summarized here. Six steps are taken to establish the elements of the power flow analysis.

The derivation of the power flow analysis model of the microgrid rests in the recognition that the production system acts as a load on the microgrid and must be included. The first step specifies a device model for every structural degree of freedom in J_{MPS}. In the device model, the set of algebraic state variables is defined as $w_{E\psi} = [P_\psi, Q_\psi, v_\psi, \theta_\psi]$, where

- P_ψ – is active power injection from ground.

- Q_ψ – is the associated reactive power injection from ground.

- v_ψ – is the associated voltage magnitude relative to ground.

- θ_ψ – is the associated voltage angle relative to a predefined reference bus.

For each structural degree of freedom ψ [48], the device model for transportation structural degrees of freedom contains a specific set of algebraic equations:

$$g_\psi = P_{E_\psi} + jQ_\psi = (v_\psi \angle \theta_\psi) y_\psi^* (v_\psi \angle \theta_\psi)^* \tag{32}$$

In the second step, for convenience, the transportation degrees of freedom $\mathcal{E}_{\psi H}$ are distinguished from the transformation degrees of freedom $\mathcal{E}_{\psi M}$. Each element in the transportation structural degrees of freedom is also assigned an admittance $y_{\psi h}$. These are organized into a transportation degree of freedom admittance matrix, which can be compared with the line admittance matrix in traditional power flow analysis [48].

$$\mathcal{Y} = diag(y_{\psi h_1}, ..., y_{\psi h_{\sigma(2H)}}) \tag{33}$$

The third step defines the transportation degree of freedom incidence matrix $M_{\mathcal{E}_{\psi H}}$, using Equations 4 and 5. The transportation degree of freedom incidence matrix can be compared with the bus incidence matrix in traditional power flow analysis [48].

$$M_{\mathcal{E}_{\psi H}} = M_{\mathcal{E}_{\psi H}}^+ - M_{\mathcal{E}_{\psi H}}^- \tag{34}$$

where

$$M_{\mathcal{E}_{\psi H}}^- = \sum_{y1=1}^{\sigma(B_{S_{MPS}})} e_{y1}^{\sigma(B_{S_{MPS}})} [\mathbb{P}_H(X_{y_1}^-)^V]^T \tag{35}$$

16

Figure 2: Petri Net Graph of the Starling Manufacturing System.

Resources:
M1 - Milling Station 1
M2 - Assembly Station 1
M3 - Painting Station 1
M4 - Milling Station 2
M5 - Assembly Station 2
M6 - Painting Station 2
B1 - Input Buffer
B2 - Output Buffer
S1 - Shuttle 1
S2 - Shuttle 2

Transitions:
t1 - Lathe Cylinder Tab, by resource M1
t2 - Lathe Cylinder Slot, by resource M1
t3 - Mill Cylinder Hole, by resource M1
t4 - Buffering process, by resource M1
t5 - Buffering process, by resource M1
t6 - Assembly process, by resource M2
t7 - Buffering process, by resource M2
t8 - Buffering process, by resource M2
t9 - Paint Yellow, by resource M3
t10 - Paint Green, by resource M3
t11 - Paint Blue, by resource M3
t12 - Buffering process, by resource M3
t13 - Lathe Cylinder Tab, by resource M4
t14 - Lathe Cylinder Slot, by resource M4
t15 - Mill Cylinder Hole, by resource M4
t16 - Buffering process, by resource M4
t17 - Buffering process, by resource M4
t18 - Assembly process, by resource M5
t19 - Buffering process, by resource M5
t20 - Buffering process, by resource M5
t21 - Paint Green, by resource M6
t22 - Paint Yellow, by resource M6
t23 - Paint Blue, by resource M6
t24 - Buffering process, by resource M6
t25 - Buffering process, by resource B1
t26 - Buffering process, by resource B2

Transitions:
t27 - Transport process, by Shuttle 1
t28 - Transport process, by Shuttle 1
t29 - Transport process, by Shuttle 1
t30 - Transport process, by Shuttle 1
t31 - Transport process, by Shuttle 1
t32 - Transport process, by Shuttle 1
t33 - Transport process, by Shuttle 1
t34 - Transport process, by Shuttle 1
t35 - Transport process, by Shuttle 1
t36 - Transport process, by Shuttle 1
t37 - Transport process, by Shuttle 1
t38 - Transport process, by Shuttle 1
t39 - Transport process, by Shuttle 1
t40 - Transport process, by Shuttle 1
t41 - Transport process, by Shuttle 1
t42 - Transport process, by Shuttle 1
t43 - Transport process, by Shuttle 1

Transitions:
t44 - Transport process, by Shuttle 1
t45 - Transport process, by Shuttle 1
t46 - Transport process, by Shuttle 1
t47 - Transport process, by Shuttle 1
t48 - Transport process, by Shuttle 1
t49 - Transport process, by Shuttle 1
t50 - Transport process, by Shuttle 1
t51 - Transport process, by Shuttle 1
t52 - Transport process, by Shuttle 1
t53 - Transport process, by Shuttle 1
t54 - Transport process, by Shuttle 1
t55 - Transport process, by Shuttle 1
t56 - Transport process, by Shuttle 1
t57 - Transport process, by Shuttle 1
t58 - Transport process, by Shuttle 1
t59 - Transport process, by Shuttle 1
t60 - Transport process, by Shuttle 1

Transitions:
t61 - Transport process, by Shuttle 1
t62 - Transport process, by Shuttle 1
t63 - Transport process, by Shuttle 1
t64 - Transport process, by Shuttle 1
t65 - Transport process, by Shuttle 1
t66 - Transport process, by Shuttle 1
t67 - Transport process, by Shuttle 1
t68 - Transport process, by Shuttle 1
t69 - Transport process, by Shuttle 1
t70 - Transport process, by Shuttle 1
t71 - Transport process, by Shuttle 1
t72 - Transport process, by Shuttle 1
t73 - Transport process, by Shuttle 1
t74 - Transport process, by Shuttle 1
t75 - Transport process, by Shuttle 1
t76 - Transport process, by Shuttle 1
t77 - Transport process, by Shuttle 1

Transitions:
t78 - Transport process, by Shuttle 1
t79 - Transport process, by Shuttle 1
t80 - Transport process, by Shuttle 1
t81 - Transport process, by Shuttle 1
t82 - Transport process, by Shuttle 1
t83 - Transport process, by Shuttle 2
t84 - Transport process, by Shuttle 2
t85 - Transport process, by Shuttle 2
t86 - Transport process, by Shuttle 2
t87 - Transport process, by Shuttle 2
t88 - Transport process, by Shuttle 2
t89 - Transport process, by Shuttle 2
t90 - Transport process, by Shuttle 2
t91 - Transport process, by Shuttle 2
t92 - Transport process, by Shuttle 2
t93 - Transport process, by Shuttle 2
t94 - Transport process, by Shuttle 2

Transitions:
t95 - Transport process, by Shuttle 2
t96 - Transport process, by Shuttle 2
t97 - Transport process, by Shuttle 2
t98 - Transport process, by Shuttle 2
t99 - Transport process, by Shuttle 2
t100 - Transport process, by Shuttle 2
t101 - Transport process, by Shuttle 2
t102 - Transport process, by Shuttle 2
t103 - Transport process, by Shuttle 2
t104 - Transport process, by Shuttle 2
t105 - Transport process, by Shuttle 2
t106 - Transport process, by Shuttle 2
t107 - Transport process, by Shuttle 2
t108 - Transport process, by Shuttle 2
t109 - Transport process, by Shuttle 2
t110 - Transport process, by Shuttle 2

Transitions:
t111 - Transport process, by Shuttle 2
t112 - Transport process, by Shuttle 2
t113 - Transport process, by Shuttle 2
t114 - Transport process, by Shuttle 2
t115 - Transport process, by Shuttle 2
t116 - Transport process, by Shuttle 2
t117 - Transport process, by Shuttle 2
t118 - Transport process, by Shuttle 2
t119 - Transport process, by Shuttle 2
t120 - Transport process, by Shuttle 2
t121 - Transport process, by Shuttle 2
t122 - Transport process, by Shuttle 2
t123 - Transport process, by Shuttle 2
t124 - Transport process, by Shuttle 2
t125 - Transport process, by Shuttle 2
t126 - Transport process, by Shuttle 2
t127 - Transport process, by Shuttle 2

Transitions:
t128 - Transport process, by Shuttle 2
t129 - Transport process, by Shuttle 2
t130 - Transport process, by Shuttle 2
t131 - Transport process, by Shuttle 2
t132 - Transport process, by Shuttle 2
t133 - Transport process, by Shuttle 2
t134 - Transport process, by Shuttle 2
t135 - Transport process, by Shuttle 2
t136 - Transport process, by Shuttle 2
t137 - Transport process, by Shuttle 2
t138 - Transport process, by Shuttle 2

with:

$$X_{y_1}^- = e_{y1}^{\sigma(B_{S_{MPS}})} \otimes \mathbb{1}^{\sigma(B_{S_{MPS}})} \otimes \mathbb{1}^{\sigma(R_{MPS})T} \tag{36}$$

and where

$$M_{\mathcal{E}_{\psi H}}^+ = \sum_{y2=1}^{\sigma(B_{S_{MPS}})} e_{y2}^{\sigma(B_{S_{MPS}})}[\mathbb{P}_H(X_{y_2}^+)^V]^T \tag{37}$$

with:

$$X_{y_2}^+ = \mathbb{1}^{\sigma(B_{S_{MPS}})} \otimes e_{y2}^{\sigma(B_{S_{MPS}})} \otimes \mathbb{1}^{\sigma(R_{MPS})T} \tag{38}$$

and where

$$\mathbb{P}_H = [e_{\psi H_1}^{\sigma(P_\eta)\sigma(H)}, \ldots, e_{\psi H_n}^{\sigma(P_\eta)\sigma(H)}] \tag{39}$$

The fourth step combines the transportation degrees of freedom admittance matrix (Equation 33) and incidence matrix (Equation 34), to calculate the bus admittance matrix with size $\sigma(B_{S_{MPS}}) \times \sigma(B_{S_{MPS}})$, as traditionally defined in power systems engineering [48, 62].

$$\mathbf{Y} = M_{\mathcal{E}_{\psi H}} * \mathcal{Y} * M_{\mathcal{E}_{\psi H}}^T \tag{40}$$

The fifth step extends the previously established derivation of the power flow analysis as the term $\mathcal{M}$ is introduced to allow for multiple degrees of freedom in one system resource [48].

$$\mathcal{M}_E = \sum_{y_1=1}^{\sigma(B_S)} e_{y_1}^{\sigma(B_S)}[\mathbb{P}_M(\mathbb{1}^{\sigma(P_\mu)} e_{y_1}^{\sigma(M)})^V]^T \tag{41}$$

where

$$\mathbb{P}_M = [e_{\psi M_1}^{\sigma(P_\mu)\sigma(M)}, \ldots, e_{\psi M_n}^{\sigma(P_\mu)\sigma(M)}] \tag{42}$$

As the final step, the power flow equations follow straightforwardly from Kirchoff's Current Law [48, 62, 63].

$$\mathcal{M}_E[\mathbf{P}_E + j\mathbf{Q}] = diag(\mathbf{V})\mathbf{Y}^*\mathbf{V}^* \tag{43}$$

where P, Q are associated with transformation degrees of freedom. $\mathbf{V}$ has size $\sigma(B_{S_{MPS}}) \times \mathbf{1}$ and contains the nodal voltage levels, as defined in the device model. In such a way, the relatively abstract Axiomatic Design knowledge base is shown to be entirely consistent with traditional power flow analysis.

In conclusion, this section formulates a dynamic model for the energy management of microgrid-enabled production systems. The model is dynamic in the sense that it represents the production system's discrete event dynamics using Petri nets. It facilitates energy management in that the energy consumption of the production system is tightly integrated with the underlying microgrid.

4. Illustrative Example

This section discusses an example for a Microgrid-Enabled Production System. This specific example is chosen because it includes elements that cover all of the definitions in the microgrid-enabled production system model while still retaining enough simplicity so as to give relatively intuitive results. The production system part of the system is further detailed in Subsection 4.1. The microgrid part of the system is further detailed in Subsection 4.2.

4.1. Production System

The Starling Manufacturing System is a discrete part production system of bird feeders and depicted in Figure 3 [36, 37, 39]. It consists of ten resources; three pairs of transforming machines M_{PS} = {Machining Station 1, Assembly Station 1, Painting Station 1, Machining Station 2, Assembly Station 2, Painting Station 2}, two independent buffers B_{PS} = {Input Buffer, Output Buffer}, and two transportation resources H_{PS} = {Shuttle A, Shuttle B}. The independent buffers store product elements before and after processing in the production system. The transportation resources are shuttles that move on tracks; following the direction of the arrows (as displayed in Figure 3).
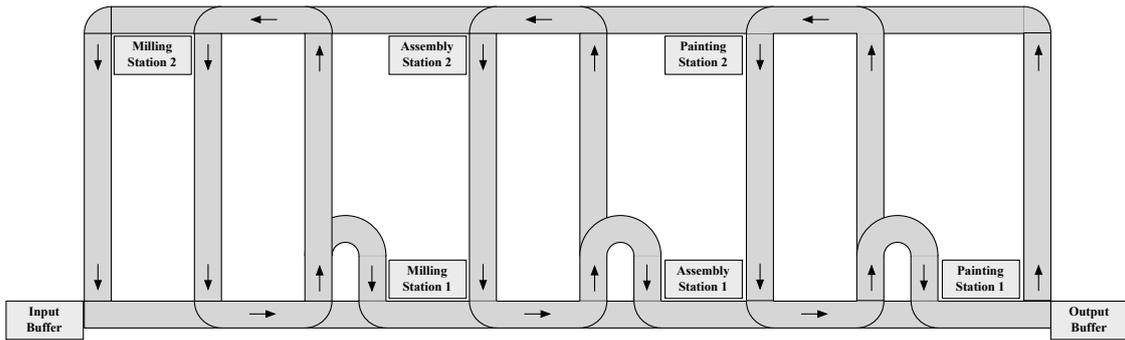
Figure 3: Starling Manufacturing System Overview

The bird feeders consist of three parts; a bottom, middle, and top cylinder. It is produced in seven transformation processes $P_{\mu PS}$ = {Lathe Tab, Lathe Slot, Mill Hole, Laminate, Paint Yellow, Paint Green, Paint Blue}. The transportation processes are $P_{\eta PS}$ = {$m_i m_j, m_i b_k, b_k m_i, b_k b_l$}$\forall i, j$ = 1, 2, 3, 4, 5, 6; k, l = 1, 2 and move the product parts between buffers. The holding processes account for three fixture configurations $P_{\gamma PS}$ = {Small Radial, Big Radial, Axial}. The allocation of the processes onto the resources using knowledge bases is demonstrated in earlier work.

Figure 2 on Page 17 shows the Petri net representation of the production system shown in Figure 3. Note that its lay-out is similar to the physical production system lay-out. The Petri net contains places for the set of buffers B_S, that are oriented in a similar way as in Figure 3. Every process is related to one of the transitions. These represent the production degrees of freedom. The incidence matrix is defined by Definition 9, or by inspection. The transitions are fired based on a scheduled events list. This events list is imported from an external source and assumed to be constant. The fired transitions are shown as a list in Table 3 on Page 20.

19

Table 3: Production System Firing Vectors [37]

List Index (rows)	Transition	# Tokens Fired	T start	T end	Transition	# Tokens Fired	Name
1	25	7					Buffer
2	72	1	1	4			Transportation
3	125	1	1	4			Transportation
4	1	1	5	8	1	1	Lathe Cylinder Tab
5	13	1	5	8	4	1	Lathe Cylinder Tab
6	2	1	8	11	2	1	Lathe Cylinder Slot
7	14	1	8	11	5	1	Lathe Cylinder Slot
8	3	1	11	14	3	1	Mill Cylinder Hole
9	15	1	11	14	6	1	Mill Cylinder Hole
10	49	1	14	18			Transportation
11	83	1	14	18			Transportation
12	6	1	18	23	10	1	Assembly Process
13	72	1	18	22			Transportation
14	125	1	18	22			Transportation
15	1	1	22	25	7	1	Lathe Cylinder Tab
16	13	1	22	25	7	1	Lathe Cylinder Tab
17	7	1					Buffer
18	2	1	25	28	8	1	Lathe Cylinder Slot
19	14	1	25	28	8	1	Lathe Cylinder Slot
20	3	1	28	31	9	1	Mill Cylinder Hole
21	15	1	28	31	9	1	Mill Cylinder Hole
22	49	1	31	35			Transportation
23	83	1	31	35			Transportation
24	6	1	35	40	11	1	Assembly Process
25	7	1					Buffer
26	72	1	35	39			Transportation
27	125	1	35	39			Transportation
28	1	1	39	42	1	1	Lathe Cylinder Tab
29	13	1	39	42	4	1	Lathe Cylinder Tab
30	35	1	40	45			Transportation
31	2	1	42	45	2	1	Lathe Cylinder Slot
32	14	1	42	45	5	1	Lathe Cylinder Slot
33	3	1	45	48	3	1	Mill Cylinder Hole
34	9	1	45	51	12	1	Paint Yellow
35	15	1	45	48	6	1	Mill Cylinder Hole
36	49	1	48	52			Transportation
37	83	1	48	52			Transportation
38	12	1					Buffer
39	6	1	52	57	10	1	Assembly Process
40	72	1	52	56			Transportation
41	125	1	52	56			Transportation
42	1	1	56	59	1	1	Lathe Cylinder Tab
43	13	1	56	59	4	1	Lathe Cylinder Tab
44	47	1	56	60			Transportation
45	6	1	57	62	11	1	Assembly Process
46	2	1	59	62	2	1	Lathe Cylinder Slot
47	14	1	59	62	5	1	Lathe Cylinder Slot
48	26	1					Buffer
49	3	1	62	65	3	1	Mill Cylinder Hole
50	15	1	62	65	6	1	Mill Cylinder Hole
51	35	1	62	67			Transportation
52	4	1					Buffer
53	49	1	65	69			Transportation
54	10	1	67	73	12	1	Paint Green
55	83	1	67	73			Transportation
56	7	1					Buffer
57	72	1	69	73			Transportation
58	6	1	71	76	10	1	Assembly Process
59	13	1	73	76	7	1	Lathe Cylinder Tab
60	47	1	73	77			Transportation
61	7	1					Buffer
62	14	1	76	79	8	1	Lathe Cylinder Slot
63	26	1					Buffer
64	15	1	79	82	9	1	Mill Cylinder Hole
65	49	1	82	86			Transportation
66	6	1	86	91	11	1	Assembly Process
67	35	1	91	96			Transportation
68	11	1	96	102	12	1	Paint Blue
69	47	1	102	106			Transportation

The product net is based on the production sequence. The different stages are represented by places and the transformations equal transitions between product places. The product net for a yellow bird feeder is shown in Figure 4. The product net dynamics are related to the firing vectors via the Production System Feasibility Matrix (Definition 16). When a product part is neither processed nor buffered, it appears as a queue in the buffer state vector Q_S. However, all places have a transition that represents the buffering process. As a result, queues only occur when the capacity of the place is exceeded. The transition state vector $Q_{\mathcal{E}}$ shows the tokens per transition. The transitions consume a predefined amount of energy, which is added to the idling consumption of the machines. Additionally, the assumption is made that the transitions related to transportation resources and independent buffers do not consume power.

4.2. Electric Power System

The microgrid lay-out is based on the microgrid in the book by Saadat [64]. The load buses are corresponding with the machines in the production system. The system consists of nine transforming or buffering resources $B_{S_{MG}}$ = {Load

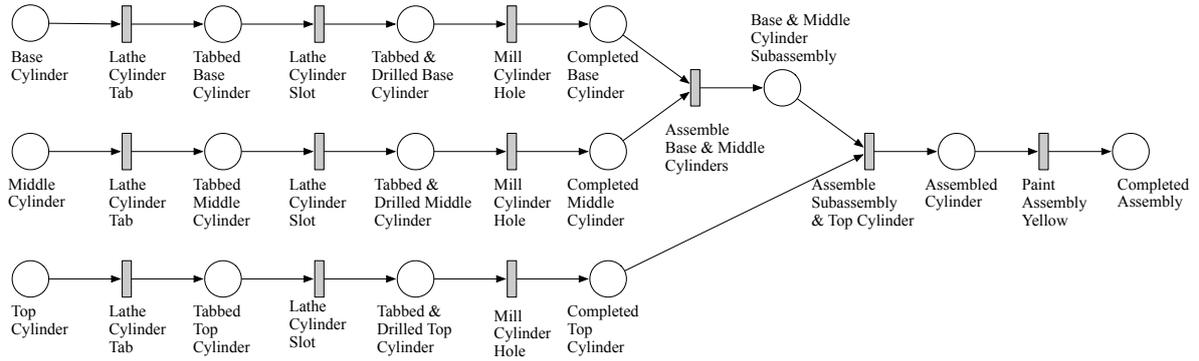Figure 4: Product net for a yellow birdfeeder [37]

Bus 1, Load Bus 2, Load Bus 3, Load Bus 4, Load Bus 5, Load Bus 6, Slack Bus, RE Generator 1, RE Generator 2}, where the Slack Bus is considered to be a dispatchable generator (i.e. a connection to the larger power grid, a battery, etc). The transportation resources are the power lines H_{MG} = {Power Line 1, . . . , Power Line 10}. This set of energy resources captures the breadth of functionality described in the Methodological Development (Section 3). The transformation processes in the system are $P_{\mu MG}$ = {Generate Power, Consume Power}. The holding processes $P_{\varphi MG}$ are assumed to be the same for every bus and every power line and can thus be neglected. The transportation processes $P_{\eta MG}$ can be derived from Figure 5, in which the arrows leaving the buses indicate the loads.
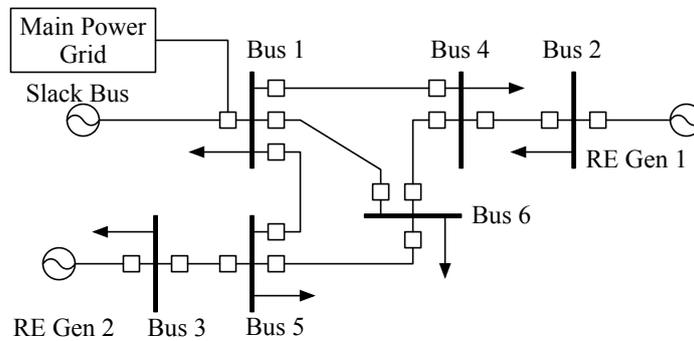
Figure 5: Overview of the Microgrid structure [64]

The input data for the renewable energy generators is generated by the DOE/NREL alliance [65]. The two renewable energy resources are assumed to be solar photovoltaics; each with a peak generation of 11.5 MW. Both the power generation and the power consumption are assumed to contain solely the active power. Figure 7 shows the energy generation curve of the generators independently and aggregated. The slack bus sustains the power balance in the microgrid and is allowed to be both positive and negative. The slack bus can, for example, be a combination of a connection with the power grid, to offload a generation surplus, and a gas turbine, to provide when there is a power

21

deficit. The gas turbine, in this illustrative example, is assumed to have a heat rate of 14,692.6 BTU/kWh at minimum efficiency, and 11,302 BTU/kWh at maximum efficiency [66, 67].

This example demonstrated the breadth of function in the methodological development (Section 3). Future work can add greater redundancy in both the production system as well as the power grid so as to more deeply investigate control and optimization decision making algorithms.

5. Results & Discussion

The Microgrid-Enabled Production System model succeeds to integrate the microgrid and the production system in one model. It aggregates both system resources and processes, which results in the shared knowledge base J_{MPS}.

The system transformation resources are M_{MPS} = {Machine 1, Machine 2, Machine 3, Machine 4, Machine 5, Machine 6, Input Buffer, Output Buffer, Shuttle 1, Shuttle 2, Slack Bus, RE Generator 1, RE Generator 2}. The system transportation resources are $H_{MPS} = H_{MG}$. The system transformation processes are $P_{\mu MPS}$ = {Lathe Tab, Lathe Slot, Mill Hole, Laminate, Paint Yellow, Paint Green, Paint Blue, $m_i m_j, m_i b_k, b_k m_i, b_k b_l$, Generate Power} $\forall i, j = 1, 2, 3, 4, 5, 6; k, l = 1, 2$. The system transportation processes $P_{\eta MPS} = P_{\eta MG}$.

Table 3 shows the transitions of the tokens in the product Petri net over time. By inspection it can be concluded that the products evolve correctly through the product net.
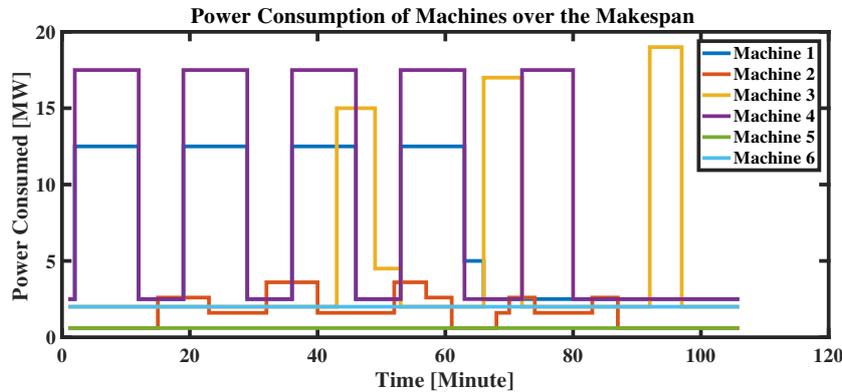
Figure 6: Energy Consumption of the Machines over Time

The transitions in the product net are coupled to the transitions in the production Petri net. Figure 6 shows the energy consumption of the production system's machine over the duration of their production schedule of 110 minutes. The energy consumption of the machines is presented in Figure 6. This figure can be compared with the product net transitions of Table 3 and by inspection the energy consumption of the machines corresponds with the evolutions of the product parts. Additionally, the transitions have different levels of energy consumption in different machines. This explains the difference in height between the curve of Machine 1 and Machine 4. Machine 5 and Machine 6 consume a constant level of energy, which is the result of standing idle.

22
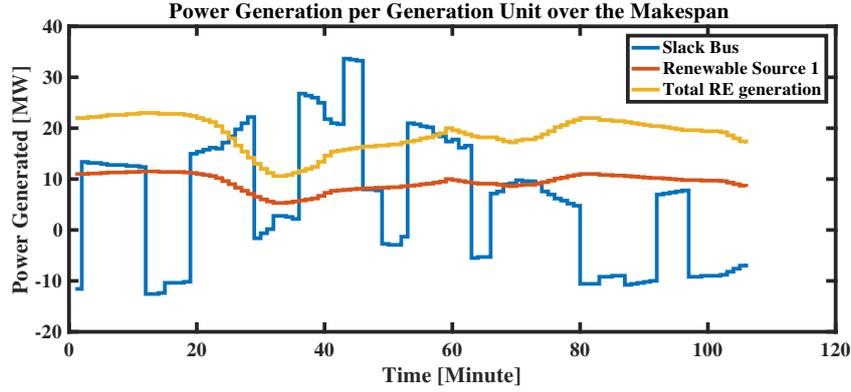
Figure 7: Energy Generation over Time

Figure 7 displays the energy generation of the three different energy sources over time. Two renewable energy sources (solar photovoltaics) are included. These generators have the same pattern and the two lines represent the individual pattern (RE. Gen. 1) and the aggregated pattern (RE. Gen. Total).

Both the renewable energy generation and the production system consumption are highly variable. The slack bus needs to match the netload of the system. This clearly shows the challenge of islanded operation of a microgrid-enabled production system, as the ramping speed of the slack bus needs to be large. To resolve this control problem, there is a clear need to decrease the variability of the production system energy consumption.

Under the assumption that the gas turbine produces the power demand that is not provided by the renewable energy resources, the CO_2 emissions can be calculated with the provided heat rate data. The heat rate decreases with more efficient operation of the gas turbine and is thus modeled as a linear function of the relative load on the turbine. The CO_2 emissions of the gas turbine are 53.07 Kilogram per 1 million BTU natural gas fed into the turbine. The CO_2 are calculated as:

$$CO_2 \text{ emissions} = \begin{pmatrix} \text{Carbon Intensity} \\ \text{of Fuel } [CO_2/\text{BTU}] \end{pmatrix} \begin{pmatrix} \text{Heat Rate} \\ [\text{BTU/MWh}] \end{pmatrix} \begin{pmatrix} \text{Electrical Energy} \\ \text{Generated } [\text{MWh}] \end{pmatrix} \tag{44}$$

The resulting rate of CO_2 emissions is presented in Figure 8.

Generally speaking, the microgrid-enabled production system model shows that the production activities can be directly coupled as a load to the microgrid. The two unlike systems come together in a model that addresses the characteristics of each of the systems. The model shows that a production system that is optimized solely for production, may impose an unwanted load on the microgrid. Consequently, grid balancing activities would need to address this variable behavior; as demonstrated in Figure 7. The determination of the firing vectors can therefore be viewed as an opportunity for decision-making that dynamically manages production activities with the energy management of the microgrid. Finally, the model can be used to create a better insight in the detailed dynamics of the microgrid (e.g. transient stability analysis) as has been demonstrated in [48].
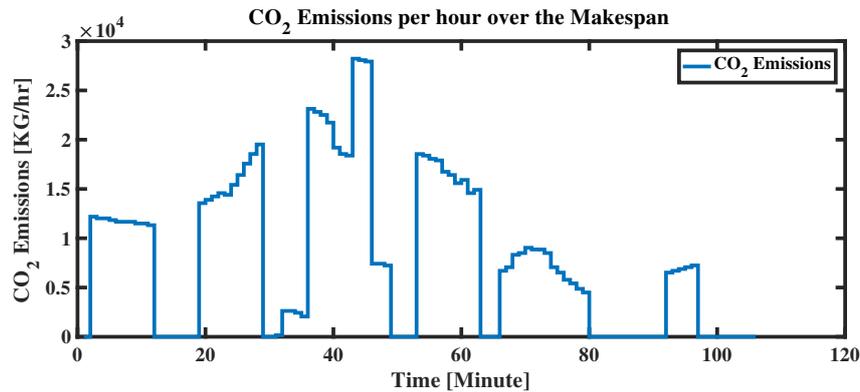
Figure 8: CO_2 emissions from the Gas Turbine over Time

6. Conclusion & Future Work

This article defines a dynamic model for the energy management of microgrid-enabled production systems. It succeeds in integrating a production system model with a power grid model, using Axiomatic Design for Large Flexible Engineering Systems. A mutually exclusive and collectively exhaustive description of processes and resources is introduced, which form the basis of precise energy accounting and accurate grid operations. The power flow analysis analyzes the static state of the power system. The outcomes of the example show that the variable electricity demand imposed by production activities is ill accommodated by the renewable energy sources alone. The slack bus is necessary to maintain the balance on the microgrid. Additionally, this model can function to calculate requirements for microgrid-enabled production facilities, more specifically energy storage and demand response. In future work, this model may be used for energy management decisions using the firing vectors that control the production system processes. Different system set ups can be compared on their electricity consumption and their microgrid impacts.

References

[1] M. Schulze, H. Nehler, M. Ottosson, P. Thollander, Energy management in industry–a systematic review of previous findings and an integrative conceptual framework, Journal of Cleaner Production 112 (2016) 3692–3708.

[2] T. Napp, A. Gambhir, T. Hills, N. Florin, P. Fennell, A review of the technologies, economics and policy instruments for decarbonising energy-intensive manufacturing industries, Renewable and Sustainable Energy Reviews 30 (2014) 616–640. doi:10.1016/j.rser.2013.10.036.

[3] A. T. de Almeida, F. J. Ferreira, D. Both, Technical and economical considerations in the application of variable-speed drives with electric motor systems, IEEE Transactions on Industry Applications 41 (1) (2005) 188–199.

[4] M. Åhman, L. J. Nilsson, Decarbonizing industry in the eu: Climate, trade and industrial policy strategies, in: Decarbonization in the European Union, Springer, 2015, pp. 92–114.

[5] M. Åhman, L. J. Nilsson, B. Johansson, Global climate policy and deep decarbonization of energy-intensive industries, Climate Policy (2016) 1–16.

[6] M. E. Porter, M. R. Kramer, The link between competitive advantage and corporate social responsibility, Harvard business review 84 (12) (2006) 78–92.

[7] A. B. Carroll, Corporate social responsibility: The centerpiece of competing and complementary frameworks, Organizational Dynamics 44 (2) (2015) 87–96.

[8] M. H. Amini, B. Nabi, M.-R. Haghifam, Load management using multi-agent systems in smart distribution network, in: Power and Energy Society General Meeting (PES), 2013 IEEE, IEEE, 2013, pp. 1–5.

[9] K. G. Boroojeni, M. H. Amini, A. Nejadpak, T. Dragicevic, S. S. Iyengar, F. Blaabjerg, A novel cloud-based platform for implementation of oblivious power routing for clusters of microgrids, IEEE Access.

[10] N. Hatziargyriou, Microgrids: Architectures and Control, Wiley IEEE Press, 2014.

[11] S. Thiede, Energy efficiency in manufacturing systems, Springer Science & Business Media, 2012.

[12] K. Tanaka, Review of policies and measures for energy efficiency in industry sector, Energy Policy 39 (10) (2011) 6532–6550.

[13] H. W. Jeon, M. Taisch, V. V. Prabhu, Modelling and analysis of energy footprint of manufacturing systems, International Journal of Production Research (ahead-of-print) (2014) 1–11.

[14] G. May, M. Taisch, D. Kelly, Enhanced energy management in manufacturing through systems integration, in: Industrial Electronics Society, IECON 2013-39th Annual Conference of the IEEE, IEEE, 2013, pp. 7525–7530.

[15] E. Giacone, S. Mancò, Energy efficiency measurement in industrial processes, Energy 38 (1) (2012) 331–345.

[16] V. V. Prabhu, D. Trentesaux, M. Taisch, Energy-aware manufacturing operations, International Journal of Production Research (2015) 1–11.

[17] Y. Mikhaylidi, H. Naseraldin, L. Yedidsion, Operations scheduling under electricity time-varying prices, International Journal of Production Research 53 (23) (2015) 7136–7157.

[18] K. G. Boroojeni, M. H. Amini, S. Iyengar, Smart grids: Security and privacy issues (2016).

[19] F. Kamyab, M. Amini, S. Sheykhha, M. Hasanpour, M. M. Jalali, Demand response program in smart grid using supply function bidding mechanism, IEEE Transactions on Smart Grid 7 (3) (2016) 1277–1284.

[20] P. Vrba, V. Marik, P. Siano, P. Leitao, G. Zhabelova, V. Vyatkin, T. Strasser, A review of agent and service-oriented concepts applied to intelligent energy systems, Industrial Informatics, IEEE Transactions on 10 (3) (2014) 1890–1903. `doi:10.1109/TII.2014.2326411`.

[21] N. Yang, D. Paire, F. Gao, A. Miraoui, Power management strategies for microgrid-A short review, in: Industry Applications Society Annual Meeting, 2013 IEEE, 2013, pp. 1–9. `doi:10.1109/IAS.2013.6682500`.

[22] C.-X. Dou, B. Liu, Multi-agent based hierarchical hybrid control for smart microgrid, IEEE Transactions on Smart Grid 4 (2) (2013) 771–778. `doi:10.1109/tsg.2012.2230197`.

[23] F. I. Hernandez, C. A. Canesin, R. Zamora, F. Martina, A. K. Srivastava, Energy management and control for islanded microgrid using multi-agents, 2013 North American Power Symposium (NAPS) (2013) 1–6`doi:10.1109/naps.2013.6666963`.

[24] M. Mazidi, A. Zakariazadeh, S. Jadid, P. Siano, Integrated scheduling of renewable generation and demand response programs in a microgrid, Energy Conversion and Management 86 (0) (2014) 1118 – 1127.

[25] Z. Jun, L. Junfeng, W. Jie, H. Ngan, A multi-agent solution to energy management in hybrid renewable energy generation system, Renewable Energy 36 (5) (2011) 1352–1363. `doi:10.1016/j.renene.2010.11.032`.

[26] L. Olatomiwa, S. Mekhilef, M. Ismail, M. Moghavvemi, Energy management strategies in hybrid renewable energy systems: A review, Renewable and Sustainable Energy Reviews 62 (2016) 821–835.

[27] P. Siano, Demand response and smart grids—a survey, Renewable and Sustainable Energy Reviews 30 (2014) 461–478.

[28] P. Palensky, D. Dietrich, Demand Side Management: Demand Response, Intelligent Energy Systems, and Smart Loads (2011). `doi:10.1109/TII.2011.2158841`.

[29] V. V. Prabhu, H. W. Jeon, M. Taisch, Simulation modelling of energy dynamics in discrete manufacturing systems, in: Service Orientation in Holonic and Multi Agent Manufacturing and Robotics, Springer, 2013, pp. 293–311.

[30] B. Vogel-Heuser, B. Weißenberger, H. Meyer, J. Plössnig, Modeling of power consumption in manufacturing: Gross and detailed planning in consideration of all forms of energy as planning resources including load management during runtime, in: Industrial Technology (ICIT), 2014 IEEE International Conference on, IEEE, 2014, pp. 659–663.

[31] L. Hu, C. Peng, S. Evans, T. Peng, Y. Liu, R. Tang, A. Tiwari, Minimising the machining energy consumption of a machine tool by sequencing

the features of a part, Energy.

[32] C. Pach, T. Berger, Y. Sallez, D. Trentesaux, Reactive control of overall power consumption in flexible manufacturing systems scheduling: A potential fields model, Control Engineering Practice 44 (2015) 193–208.

[33] F. Tonelli, A. Bruzzone, M. Paolucci, E. Carpanzano, G. Nicolò, A. Giret, M. Salido, D. Trentesaux, Assessment of mathematical programming and agent-based modelling for off-line scheduling: Application to energy aware manufacturing, CIRP Annals-Manufacturing Technology.

[34] A. Giret, D. Trentesaux, V. Prabhu, Sustainability in manufacturing operations scheduling: a state of the art review, Journal of Manufacturing Systems 37 (2015) 126–140.

[35] M. Kivelä, A. Arenas, M. Barthelemy, J. P. Gleeson, Y. Moreno, M. A. Porter, Multilayer networks, Journal of complex networks 2 (3) (2014) 203–271.

[36] A. M. Farid, Static Resilience of Large Flexible Engineering Systems: Axiomatic Design Model and Measures, IEEE Systems Journal PP (99) (2015) 1–12.
URL http://dx.doi.org/10.1109/JSYST.2015.2428284

[37] A. M. Farid, Reconfigurability Measurement in Automated Manufacturing Systems, Ph.d. dissertation, University of Cambridge Engineering Department Institute for Manufacturing (2007).

[38] A. M. Farid, Product Degrees of Freedom as Manufacturing System Reconfiguration Potential Measures, International Transactions on Systems Science and Applications 4 (3) (2008) 227–242.

[39] A. M. Farid, D. C. McFarlane, Production degrees of freedom as manufacturing system reconfiguration potential measures, Proceedings of the Institution of Mechanical Engineers, Part B (Journal of Engineering Manufacture) 222 (B10) (2008) 1301–1314. doi:10.1243/09544054JEM1056.

[40] A. M. Farid, N. P. Suh, Axiomatic Design in Large Systems: Complex Products, Buildings and Manufacturing Systems, Springer, Berlin, Heidelberg, 2016.
URL http://dx.doi.org/10.1007/978-3-319-32388-6

[41] A. M. Farid, An engineering systems introduction to axiomatic design, in: A. M. Farid, N. P. Suh (Eds.), Axiomatic Design in Large Systems: Complex Products, Buildings & Manufacturing Systems, Springer, Berlin, Heidelberg, 2016, Ch. 1, pp. 1–47.
URL http://dx.doi.org/10.1007/978-3-319-32388-6

[42] A. M. Farid, Measures of Reconfigurability & Its Key Characteristics in Intelligent Manufacturing Systems, Journal of Intelligent Manufacturing 1 (1) (2014) 1–26. doi:10.1007/s10845-014-0983-7.

[43] A. Viswanath, A. M. Farid, A Hybrid Dynamic System Model for the Assessment of Transportation Electrification, in: American Control Conference 2014, 2014, pp. 1–7.

[44] A. Viswanath, E. E. S. Baca, A. M. Farid, An Axiomatic Design Approach to Passenger Itinerary Enumeration in Reconfigurable Transportation Systems, IEEE Transactions on Intelligent Transportation Systems 15 (3) (2014) 915 – 924.

[45] A. M. Farid, Electrified transportation system performance: Conventional vs. online electric vehicles, in: N. P. Suh, D. H. Cho (Eds.), Electrification of Ground Transportation Systems for Environment and Energy Conservation, MIT Press, 2015, Ch. 22, pp. 1–25.

[46] A. M. Farid, A Hybrid Dynamic System Model for Multi-Modal Transportation Electrification, IEEE Transactions on Control System Technology PP (99) (2016) 1–12.
URL http://dx.doi.org/10.1109/TCST.2016.2579602

[47] W. N. Lubega, A. M. Farid, A Reference System Architecture for the Energy-Water Nexus, IEEE Systems Journal PP (99) (2014) 1–11.

[48] A. M. Farid, Multi-Agent System Design Principles for Resilient Coordination & Control of Future Power Systems, Intelligent Industrial Systems 1 (1) (2015) 1–9.

[49] A. M. Farid, L. Ribeiro, An Axiomatic Design of a Multi-Agent Reconfigurable Mechatronic System Architecture, IEEE Transactions on Industrial Informatics 1 (1) (2015) 1–10.

[50] A. M. Farid, An Axiomatic Design Approach to Non-Assembled Production Path Enumeration in Reconfigurable Manufacturing Systems,

in: 2013 IEEE International Conference on Systems Man and Cybernetics, 2013, pp. 1–8.

[51] N. P. Suh, Axiomatic Design: Advances and Applications, Oxford University Press, 2001.

[52] T. Weilkiens, Systems engineering with SysML/UML modeling, analysis, design, Morgan Kaufmann, Burlington, Mass., 2007.

[53] C. G. Cassandras, S. Lafortune, Introduction to Discrete Event Systems, 2nd Edition, Springer, New York, NY, USA, 2007.

[54] L. Popova-Zeugmann, Time Petri Nets, Springer, 2013.

[55] W. Reisig, Understanding Petri Nets, Vol. 4, Springer, 2013.

[56] A. M. Farid, Facilitating ease of system reconfiguration through measures of manufacturing modularity, Proceedings of the Institution of Mechanical Engineers, Part B (Journal of Engineering Manufacture) – invited paper 222 (B10) (2008) 1275–1288. doi:10.1243/09544054JEM1055.

[57] V. Introna, V. Cesarotti, M. Benedetti, S. Biagiotti, R. Rotunno, Energy Management Maturity Model: an organizational tool to foster the continuous reduction of energy consumption in companies, Journal of Cleaner Production 83 (0) (2014) 108–117. doi:http://dx.doi.org/10.1016/j.jclepro.2014.07.001.
URL http://www.sciencedirect.com/science/article/pii/S0959652614006817

[58] W. C. H. Schoonenberg, A. M. Farid, A dynamic production model for industrial systems energy management, in: 2015 IEEE International Conference on Systems Man and Cybernetics, 2015, pp. 1–7.

[59] M. Zhou, N. Wu, System modeling and control with resource-oriented Petri nets, CRC Press, 2010.

[60] M. Zhou, F. Di-C, et al., Petri net synthesis for discrete event control of manufacturing systems, Kluwer Academic Publishers, 1993.

[61] K. A. D'Souza, S. K. Khator, A survey of Petri net applications in modeling controls for automated manufacturing systems, Computers in Industry 24 (1) (1994) 5–16. doi:http://dx.doi.org/10.1016/0166-3615(94)90004-3.
URL http://www.sciencedirect.com/science/article/pii/0166361594900043

[62] J. L. Kirtley, Electric power principles: sources, conversion, distribution and use, John Wiley & Sons, 2011.

[63] F. Milano, Power system modelling and scripting, 1st Edition, Springer, New York, 2010.
URL http://www.uclm.es/area/gsee/web/Federico/psat.htm

[64] H. Saadat, Power System Analysis, McGraw-Hill, 1999.

[65] Solar power data for integration studies [online] (April 2014) [cited 07-26-2015].

[66] U.S.Energy-Information-Administration. Average tested heat rates by prime mover and energy source [online] (2015).

[67] L. Danny Harvey, Energy efficiency and the demand for energy services (2010).